Gascooke, J.R., Alexander, U.N. and Lawrance, W.D., 2012. Intermolecular vibrations of fluorobenzene-Ar up to 130 cm-1 in the ground electronic state. Journal of Chemical Physics, 137, 084305.

DOI: http://dx.doi.org/10.1063/1.4746688

Intermolecular vibrations of fluorobenzene-Ar up to 130 cm−1 in the ground electronic state

Jason R. Gascooke, Ula N. Alexander, and Warren D. Lawrance

Citation: J. Chem. Phys. **137**, 084305 (2012); doi: 10.1063/1.4746688
View online: http://dx.doi.org/10.1063/1.4746688
View Table of Contents: http://jcp.aip.org/resource/1/JCPSA6/v137/i8
Published by the American Institute of Physics.

Intermolecular vibrations of fluorobenzene-Ar up to 130 cm^{-1} in the ground electronic state

Jason R. Gascooke, Ula N. Alexander, and Warren D. Lawrance[a)]
School of Chemical and Physical Sciences, Flinders University, GPO Box 2100 Adelaide, South Australia 5001, Australia

(Received 26 April 2012; accepted 2 August 2012; published online 24 August 2012)

Sixteen intermolecular vibrational levels of the S_0 state of the fluorobenzene-Ar van der Waals complex have been observed using dispersed fluorescence. The levels range up to ~130 cm^{-1} in vibrational energy. The vibrational energies have been modelled using a complete set of harmonic and quartic anharmonic constants and a cubic anharmonic coupling between the stretch and long axis bend overtone that becomes near ubiquitous at higher energies. The constants predict the observed band positions with a root mean square deviation of 0.04 cm^{-1}. The set of vibrational levels predicted by the constants, which includes unobserved bands, has been compared with the predictions of *ab initio* calculations, which include all vibrational levels up to 70–75 cm^{-1}. There are small differences in energy, particularly above 60 cm^{-1}, however, the main differences are in the assignments and are largely due to the limitations of assigning the *ab initio* wavefunctions to a simple stretch, bend, or combination when the states are mixed by the cubic anharmonic coupling. The availability of these experimental data presents an opportunity to extend *ab initio* calculations to higher vibrational energies to provide an assessment of the accuracy of the calculated potential surface away from the minimum. The intermolecular modes of the fluorobenzene-Ar_2 trimer complex have also been investigated by dispersed fluorescence. The dominant structure is a pair of bands with a ~35 cm^{-1} displacement from the origin band. Based on the set of vibrational modes calculated from the fluorobenzene-Ar frequencies, they are assigned to a Fermi resonance between the symmetric stretch and symmetric short axis bend overtone. The analysis of this resonance provides a measurement of the coupling strength between the stretch and short axis bend overtone in the dimer, an interaction that is not directly observed. The coupling matrix elements determined for the fluorobenzene-Ar stretch-long axis bend overtone and stretch-short axis bend overtone couplings are remarkably similar (3.8 cm^{-1} cf. 3.2 cm^{-1}). Several weak features seen in the fluorobenzene-Ar_2 spectrum have also been assigned. © *2012 American Institute of Physics*. [http://dx.doi.org/10.1063/1.4746688]

I. INTRODUCTION

Aromatic-rare gas van der Waals complexes have long been used as model systems for studying dispersion interactions.[1,2] *Ab initio* calculations for these systems predict the potential energy surface and hence the geometry, dissociation energy, and intermolecular vibrational levels. The intermolecular vibrational levels are sensitive to the shape of the potential energy surface and comparing the predicted levels with those observed gives insight into the accuracy of the calculated surface. This is particularly the case as the energy rises and the surface is increasingly being sampled far from the minimum.

Primarily as a result of mass-resolved resonance enhanced multiphoton ionisation (REMPI) experiments, data are available concerning the van der Waals vibration fundamentals and bend overtones in the excited electronic S_1 states of many systems. There are limited data for higher lying overtones and combinations. A notable exception is the case of *p*-difluorobenzene-Ar where a number of S_1 vibrational levels have been observed up to ~125 cm^{-1} (Ref. 3). In contrast, there is a paucity of experimental data for ground electronic S_0 states. This is unfortunate given that *ab initio* calculations are expected to be more accurate for the ground electronic state. One of the most comprehensive studies of the S_0 intermolecular vibrations of aromatic-containing complexes is due to Maxton *et al.*[4] These authors used a stimulated Raman technique to probe the bend vibrations in a series of complexes involving aromatics clustered with rare gases, diatomics, and polyatomics. Their technique was primarily sensitive to bend/libration fundamentals and hence did not provide insight into stretch or overtone levels. High resolution coherent ion dip spectroscopy[5,6] and ionisation detected stimulated Raman spectroscopy[7] have been used to observe ro-vibrational states of benzene-Ar with up to 130 cm^{-1} of intermolecular energy. Sussmann *et al.* reported that the frequency positions of the intermolecular vibrational states display a regular pattern up to the 130 cm^{-1} limit of their observations.[5]

Fluorobenzene-Ar (FB-Ar) has the distinction of being one of the few aromatic-rare gas van der Waals complexes for which there are high level *ab initio* calculations for both the S_0 and S_1 states.[8–10] We have recently reported a two-dimensional laser induced fluorescence (2D-LIF) study of

a)Author to whom correspondence should be addressed. Electronic mail: warren.lawrance@flinders.edu.au.

FB-Ar that provided insight into the S_0 intermolecular vibrational levels of the complex up to ~65 cm^{-1}, just below the limit of the reported *ab initio* calculated energy levels.[11] The 2D-LIF technique involves measuring a section of the dispersed fluorescence spectrum whilst scanning a laser over features of the absorption spectrum.[12,13] The FB-Ar study illustrated the possibilities provided by dispersed fluorescence spectra for revealing the S_0 intermolecular vibrations.

In the present work we report the results of a dispersed fluorescence study of FB-Ar. Single photon imaging has been used to record short (~80 cm^{-1}) segments of the spectrum at each laser shot. The multiplex advantage this provides over conventional photomultiplier detection makes it possible to observe the weak transitions terminating in van der Waals vibrations in the ground electronic state. The spectra reveal transitions terminating in levels with up to ~130 cm^{-1} of van der Waals mode energy. This is significantly above both our previous work and the limits of reported *ab initio* calculations.[8,9,11]

FB-Ar was the subject of this study for several reasons. First, as noted above, the results of high level *ab initio* calculations have been reported for this complex[8–10] and the experimental data provide a test of their accuracy. Second, the *ab initio* calculations reveal a strong interaction between the stretch and long axis bend overtone that we observed at the stretch fundamental previously.[9] Bieske *et al.* have suggested that such an interaction should be ubiquitous in aromatic-rare gas complexes.[14] We wished to explore its manifestation in the spectra at higher energies. Third, Makarewicz noted that his calculated energy levels were far from harmonic and suggested that the usual spectroscopic approaches for characterising the states would be inappropriate.[9] This contrasts with the benzene-Ar situation, where the states were reported to display a regular pattern up to 130 cm^{-1} (Ref. 5). We wished to explore the extent to which standard spectroscopic approaches are able to rationalise the structure observed in the FB-Ar dispersed fluorescence spectra.

While FB-Ar is the primary focus of this work, we have also obtained dispersed fluorescence spectra for FB-Ar_2 and observed several van der Waals vibrations. The interest in this trimer complex derives from the formulae relating its vibrational frequencies and anharmonic coupling matrix elements to those of the FB-Ar dimer.[15] An analysis of the trimer spectrum provides both a test of these formula and an opportunity to extract otherwise unobserved dimer coupling strengths.

II. EXPERIMENTAL DETAILS

The experimental setup is similar to that for our 2D-LIF experiment, which has been given in detail in previous publications.[11,13] The salient features for the present experiments are as follows. The frequency doubled output of a Nd:YAG pumped dye laser (coumarin 503 laser dye; 0.3 cm^{-1} doubled line width; 10 Hz repetition rate) is passed vertically through a stainless steel chamber containing the pulsed nozzle source, the vertical propagation matching the vertical entrance slit of the spectrometer. The laser beam intersects a horizontal supersonic free jet expansion of 1% FB in Ar at X/D ~ 10. The laser pulse is fired at a delay time chosen to minimise the signal from higher order clusters, whose signature is a broad feature underlying the absorption region[16] that would contribute to the background in our fluorescence spectra. The fluorescence is dispersed using a home-built spectrometer with a dispersion of ~5 cm^{-1} per mm in the wavelength region of the present experiments. The dispersed fluorescence is detected with a 25 mm diameter gated image intensifier with single photon detection sensitivity. The loss of sensitivity at the edges (due to the image intensifier vertical dimension no longer matching the slit height) leads to the effective width of the region viewed being ~80–100 cm^{-1}. The image intensifier is gated to detect fluorescence in a time window immediately following the laser pulse to minimise scattered laser light. The image intensifier output at each laser shot is captured using a charge coupled device (CCD) camera. The CCD image is downloaded to a computer and analysed to identify and record the centre of each spot observed and a histogram of events at each camera pixel position is built up.

The process described above continues for a preset number of laser shots, producing a 80–100 cm^{-1} wide section of the dispersed fluorescence spectrum associated with the absorption feature excited at the chosen laser wavelength. To measure longer sections of the dispersed fluorescence spectrum, the spectrometer wavelength region being observed was adjusted by rotating the grating and the total spectrum pieced together from the resulting segments. The segments were overlapped to include common features. When merged, the segments were set to retain the same intensity in the common features. Because a section of dispersed fluorescence is collected at each laser shot, laser intensity changes do not affect the fidelity of the spectrum and there is excellent reproducibility in the relative intensity of features.

III. RESULTS

Figure 1(a) shows the FB-Ar $\overline{0^0}$ dispersed fluorescence spectrum in the low displacement region where transitions to S_0 van der Waals vibrations occur.[11] (FB levels and transitions are shown with no bar, FB-Ar transitions with a single bar, and FB-Ar_2 transitions with a double bar.) The spectrum shown is a composite of three separately acquired segments. The parent FB spectrum is well known[17] and there are no FB vibrations with low enough energy to contribute in the region displayed in Fig. 1.

The intensities of the van der Waals bands are a few percent of the $\overline{0^0_0}$ band at best, and it is essential to distinguish the van der Waals vibrational features from experimental artefacts, particularly grating ghosts, which also occur in this region. A "spectrum" associated with scattered laser light was collected and is shown in Fig. 1(c). It can be seen that several features in the $\overline{0^0}$ spectrum arise from grating ghosts. The grating ghost spectrum was used as an instrument response function and convoluted with a series of bands to generate a spectrum for comparison with the observed $\overline{0^0}$ spectrum. By non-linear least squares fitting the calculated and observed spectra, the van der Waals bands and their relative intensity have been determined. The fitted, calculated spectrum is shown in Fig. 1(b) and the bands extracted are listed in Table I. The match between the calculated and observed spectra is

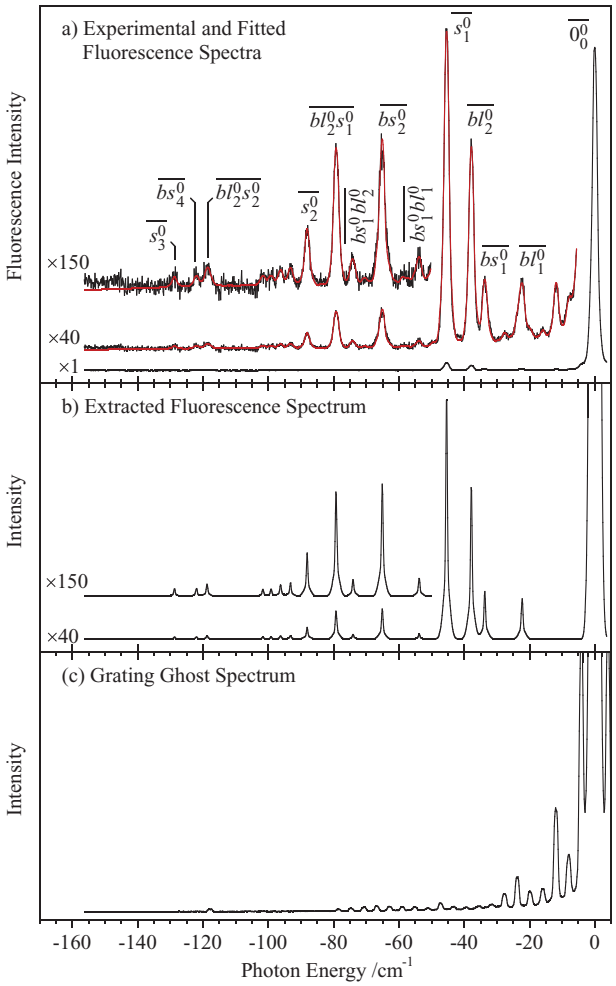

FIG. 1. (a) Dispersed fluorescence spectrum of fluorobenzene-Ar after excitation of the $\overline{0_0^0}$ transition at 37790.7 cm^{-1}. The red line represents the fit to the spectrum used to determine the position and intensity of each peak. The assignments represent transitions involving zero-order states (see text and Table I). (b) A simulated spectrum derived from the experimental data. This spectrum, convoluted with the grating ghost spectrum produced by the excitation laser, resulted in the best fit to the experimental data in the top panel. (c) The spectrum associated with scattered light at 37790.7 cm^{-1} showing the position and intensity of grating ghosts. The spectra shown in (a) and (c) were acquired in three segments. The spectra are displayed as displacement from the excitation position to show the vibrational wavenumber associated with the terminating S_0 levels. The spectrum was measured with a FWHM resolution of 1.6 cm^{-1}.

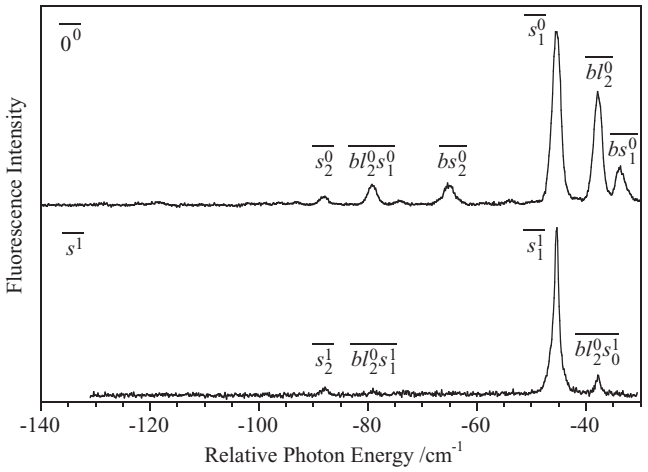

FIG. 2. The dispersed fluorescence spectra recorded from the $\overline{0^0}$ level (upper trace) and the $\overline{s^1}$ level (lower trace). The spectra are displayed as displacement from the excitation wavenumber to show the alignment of terminating S_0 levels seen in the two spectra. The upper trace is a reproduction of Fig. 1(a). The lower trace is recorded after excitation of the $\overline{s_0^1}$ transition at 37834.2 cm^{-1} and was measured with a FWHM resolution of 0.3 cm^{-1}. The assignments represent transitions involving zero-order states (see text for details).

excellent, with several features in the spectrum being well reproduced by the inclusion of grating ghosts in the fit.

The quality of the spectrum and the fit is very good and enables 12 bands to be securely identified up to 130 cm^{-1}. The fit reveals two areas where it is clear that a number of weak bands are contributing to broad features. In the region from 92 to 104 cm^{-1} there is a weak, broad feature that we have fitted to four bands, bringing the total number of bands extracted to 16. While the simulations with the four bands give a good fit to this region, this represents the minimum number required and there may be more weak bands also contributing. From 104 to 116 cm^{-1} we have omitted features for the purpose of the fit but a close examination of the spectrum suggests that there are at least 3–4 very weak transitions in this region.

A dispersed fluorescence spectrum has also been recorded following excitation of the FB-Ar van der Waals stretch vibration in S_1 (i.e., the $\overline{s^1}$ level). This is shown in Fig. 2 along with the $\overline{0^0}$ spectrum to show the alignment of S_0 levels. The spectrum clearly shows that the ground state level at 45.4 cm^{-1} has the most overlap with $\overline{s^1}$. On the face of it, this indicates that it is the $\overline{s_1}$ level. However, as shown in our earlier report, the bend overtone and stretch fundamental are involved in a Fermi resonance in both the S_1 and S_0 states, which leads to the emitting and terminating levels each being mixtures of these two zero-order states.[11] The observation that the level assigned as $\overline{s^1}$ overlaps strongly with the 45.4 cm^{-1} band in S_0 is more correctly expressed as indicating that the vibrational wavefunctions for "$\overline{s^1}$" and the 45.4 cm^{-1} band in S_0 are similar, leading to strong overlap. It is interesting to note that the two transitions to the stretch overtone region near 80–90 cm^{-1} have different relative intensities in emission from $\overline{s^1}$ compared with $\overline{0^0}$. This is discussed in Sec. IV A 2.

IV. DISCUSSION

A. van der Waals vibrational structure of S_0 FB-Ar

The vibrational structure associated with the intermolecular potential of a van der Waals complex provides important information about the shape of the potential energy surface. Consequently, *ab initio* studies have been undertaken to predict the vibrational structure for FB-Ar for the lower part of the potential well.[8,9] However, prior to the present work only five vibrational levels had been reported for S_0 FB-Ar, giving limited data to test these predictions.[4,11] This situation is a general one for these types of van der Waals complexes, primarily because of the comparative complexity of the

TABLE I. The band positions and their relative intensities extracted from the fit to the dispersed fluorescence spectrum after excitation of the $\overline{0_0^0}$ transition of fluorobenzene-argon (see Fig. 1). The energy levels determined from previous experimental studies are included for comparison. Also displayed are the assignments of the features in the dispersed fluorescence spectrum and their calculated energies based on the spectroscopic constants listed in Table II.

Current work		Previous work		Assignment[d]		Calculated[g]	
Observed transition energy[a]/cm^{-1}	Intensity/ arbitrary units	Maxton *et. al.*[b] energy/cm^{-1}	Gascooke *et al.*[c] energy/cm^{-1}	Transition[e]	Terminating vibrational level[f]	Linear combination[h]	Energy/ cm^{-1}
0	1000	...	...	$\overline{0_0^0}$	(0, 0, 0)	...	0
−22.3	4.1	22.5	22.3	$\overline{bl_1^0}$	(0, 1, 0)	...	22.3
−33.7	4.8	33.5	33.6	$\overline{bs_1^0}$	(1, 0, 0)	...	33.7
−37.8	16		37.6	$\overline{bl_2^0}$	(0, 2, 0)	$-0.69\|0, 0, 1\rangle + 0.73\|0, 2, 0\rangle$	37.8
−45.4	25		45.4	$\overline{s_1^0}$	(0, 0, 1)	$0.73\|0, 0, 1\rangle + 0.69\|0, 2, 0\rangle$	45.4
−53.8	0.50			$\overline{bs_1^0 bl_1^0}$	(1, 1, 0)	...	53.8
−65.1	3.0		65.0	$\overline{bs_2^0}$	(2, 0, 0)	...	65.2
−74.0	0.46			$\overline{bs_1^0 bl_2^0}$	(1, 2, 0)	$0.66\|1, 0, 1\rangle + 075\|1, 2, 0\rangle$	74.0
−79.2	2.9			$\overline{bl_2^0 s_1^0}$	(0, 2, 1)	$-0.73\|0, 0, 2\rangle + 0.48\|0, 2, 1\rangle + 0.48\|0, 4, 0\rangle$	79.2
−88.1	1.2			$\overline{s_2^0}$	(0, 0, 2)	$0.66\|0, 0, 2\rangle + 0.67\|0, 2, 1\rangle + 0.34\|0, 4, 0\rangle$	88.1
−93.2	0.37			Not assigned		...	
−96.3	0.31			Not assigned		...	
−99.2	0.20			Not assigned		...	
−101.7	0.19			Not assigned		...	
−118.7	0.33			$\overline{bl_2^0 s_2^0}$	(0, 2, 2)	$-0.71\|0, 0, 3\rangle + 0.42\|0, 2, 2\rangle + 0.51\|0, 4, 1\rangle + 0.23\|0, 6, 0\rangle$	118.7
−122.0	0.21			$\overline{bs_4^0}$	(4, 0, 0)	...	122.0
−128.7	0.21			$\overline{s_3^0}$	(0, 0, 3)	$0.68\|0, 0, 3\rangle + 0.62\|0, 2, 2\rangle + 0.37\|0, 4, 1\rangle + 0.13\|0, 6, 0\rangle$	128.7

[a]Values are relative to the $\overline{0_0^0}$ transition of fluorobenzene-argon located at 37790.7 cm^{-1}.
[b]Stimulated Raman study (Ref. 4).
[c]Two-dimensional laser induced fluorescence study (Ref. 11).
[d]For states involved in the Fermi resonance, the assignment refers to the zero order state from which the molecular state is derived based on its position in the coupling matrix. The vibrations are better described as mixed states due to coupling between the long axis bend and stretch vibrations (see text).
[e]Vibrational modes are the short axis bend, *bs*, the long axis bend, *bl*, and the stretch, *s*.
[f]States are given in the form ($\upsilon_{\text{short bend}}$, $\upsilon_{\text{long bend}}$, $\upsilon_{\text{stretch}}$).
[g]Values calculated using the spectroscopic constants determined from this study, including anharmonic coupling (see Table II).
[h]For states involved in the Fermi resonances, this column shows the linear combination as determined by the eigenvectors of the coupling matrix.

multiple-laser experimental methods that have typically been used to observe these transitions.

The FB-Ar van der Waals complex has three intermolecular vibrational modes. These are the stretch, denoted by *s*, the long axis bend, *bl*, and the short axis bend, *bs*. The long axis bend is the bend in the C-F bond direction while the short axis bend is perpendicular to it. Maxton *et al.* provided a significant study of S_0 van der Waals vibrations in a series of aromatic-rare gas complexes, including FB-Ar (Ref. 4). Their Raman technique is primarily sensitive to bend motions and for FB-Ar they observed the long and short axis bend fundamentals, which they reported as $\nu_{bl} = 22.5$ cm^{-1} and $\nu_{bs} = 33.5$ cm^{-1}. Using 2D-LIF we have previously reported observing these two fundamentals at $\nu_{bl} = 22.3$ cm^{-1} and $\nu_{bs} = 33.6$ cm^{-1}, along with their first overtones ($2\nu_{bl} = 37.6$ cm^{-1} and $2\nu_{bs} = 65.0$ cm^{-1}), and the stretch fundamental ($\nu_s = 45.4$ cm^{-1}).[11]

Interestingly, while the long axis bend and the stretch fundamentals are symmetry allowed, the short axis bend is symmetry forbidden. Such behaviour has been observed previously and ascribed to various effects. Sussmann *et al.* reported that the equivalent mode in the closely related *p*-difluorobenzene-Ar system is active due to a Herzberg-Teller vibronic coupling mechanism.[18] These authors went on to reassign the 34 cm^{-1} van der Waals absorption feature seen in the fluorobenzene-Ar REMPI spectrum to the short axis bend fundamental.[18] However, Maxton *et al.* describe an alternative mechanism by which the van der Waals vibrations can gain transition intensity.[4] In essence, they show that the libration (rocking) of the aromatic associated with bending motion can modulate the projection of the aromatic-localised transition dipole along the Eckart axes of the complex. In the case of FB-Ar, the rocking motion of FB associated with the short axis bend effectively projects the transition dipole, μ, which is in-plane and perpendicular to the C-F bond, onto the FB-Ar bond direction, thus producing the vibronic activity observed for the short axis bend. This mechanism can be considered within a Herzberg-Teller type expansion, where a $(\frac{\partial \mu}{\partial Q_i})_{Q_0} Q_i$ term (here Q_i represents a vibrational normal coordinate) describes the change in transition dipole with van der

Waals vibration. For this reason it has the same symmetry requirements as the conventional Herzberg-Teller formula, and is experimentally indistinguishable in terms of the rotational band structure. Thus Sussmann's observations and Maxton's rationale are consistent. One feature of Maxton's mechanism is that the relative intensity of an induced transition is readily calculated. In the case of the FB-Ar short axis bend, the calculated relative intensity is 0.0044, remarkably consistent with the value of 0.0048 observed for $\overline{bs}_1^0$ (see Table I).

Our earlier spectra revealed a strong Fermi resonance interaction between the stretch fundamental and two quanta of the long axis bend. Bieske *et al.* proposed that in aromatic-rare gas complexes the stretch fundamental and bend overtones couple through a kinetic anharmonic mechanism and that this type of interaction should be a ubiquitous feature of such systems.[14] The *ab initio* vibrational wavefunctions reveal motions that are not simple stretching and bending but are mixtures of both, illustrating that coupling is present.[8,9] Indeed, Makarewicz notes that this anharmonic coupling interaction qualitatively explains the nature of the calculated vibrational wavefunctions,[9] however, he argues that a quantitative interpretation using this approach is inappropriate.

It rapidly becomes apparent when attempting to assign the spectrum (Fig. 1) that a full spectroscopic modelling is required, where the anharmonicity of the states and the stretch-bend Fermi resonance are included. The rationalisation of molecular spectra in terms of interactions between zero-order states has a long and successful history and, while we acknowledge Makarewicz's comments,[9] it provides a natural starting point for interpreting the van der Waals intermolecular vibrational spectra observed. Since there are only three intermolecular modes, with two of them involved in a Fermi resonance interaction many of the states observed are affected. Moreover, determining a set of spectroscopic constants that accurately predict the observed band positions enables a complete set of vibrational states to be predicted within a chosen energy range for comparison with that determined by *ab initio* methods.

1. Determining the spectroscopic constants

If the van der Waals vibrational states show the behaviour typical of molecular vibrations, their energies relative to the zero point energy should be reproduced using the standard formula:[19]

$$G(\upsilon_1, \upsilon_2, \upsilon_3) = \sum_{i=1}^{3} \upsilon_i \, \omega_i + \sum_{i=1}^{3} \sum_{j \geq i}^{3} \upsilon_i \, \upsilon_j \, x_{ij}$$

Here $G(\upsilon_1, \upsilon_2, \upsilon_3)$ is the vibrational energy for the state with υ_1 quanta in the short axis bend ν_{bl}, υ_2 quanta in the long axis bend ν_{bs}, and υ_3 quanta in the stretch ν_s. Energies are measured relative to the ground state, ω_i is the harmonic frequency of mode i and x_{ij} are the anharmonic terms. It is reasonable to begin by assuming that deviations from this approach result from the resonance discussed above and that including it will account for the band energies observed. For the purposes of this discussion we introduce the notation (υ_1, υ_2, υ_3) to describe the vibrational levels associated with the van der Waals modes.

As already discussed, a strong Fermi resonance exists between the long axis bend overtone and stretch vibration leading to states of the form (υ_{bs}, υ_{bl}, υ_s) interacting with states (υ_{bs}, $\upsilon_{bl}+2$, υ_s-1). For coupled harmonic oscillators, the coupling matrix element (cubic anharmonic coupling constant) for this interaction, V, varies with the vibrational quantum numbers:[20]

$$V = V_0 \sqrt{\frac{\upsilon_s(\upsilon_{bl}+1)(\upsilon_{bl}+2)}{2}},$$

where V_0 is the value of the coupling matrix element for the interaction between two quanta of the long axis bend and one quantum of the stretch, i.e., the interaction between (0,2,0) and (0,0,1). At higher quanta, the interaction can involve a multiplet of states. For example, at the stretch overtone there is a triad of states coupled: (0,0,2) couples with (0,2,1) which in turn couples with (0,4,0). The molecular states are calculated as the eigenvalues (energies) and eigenvectors (the coefficients for the zero-order states as linear combinations to form the molecular states) of the coupling matrix.

Two issues with fitting the data are the large number of variables involved and the difficulty of assigning many of the weaker higher levels *a priori*. Consequently, we employed a sequential strategy by which we first assigned low lying levels and, based on the constants determined, predicted the next higher lying levels. This generally allowed those levels to be securely assigned and the constants refined before proceeding to the next set of levels. The fitting was performed by minimising the sum of the squares of the differences between the observed and calculated energies.

We began by fixing the anharmonic coupling constant, V_0, to the value determined by analysing the Fermi resonance at the (0,0,1)-(0,2,0) level assuming no oscillator strength for the long axis bend overtone. Based on the intensity ratio for fluorescence to (0,2,0) versus (0,0,1) and their separation, we determine V_0 to be 3.7 cm^{-1}, which compares well with the value of 3.8 cm^{-1} determined previously from the 2D-LIF spectra.[11] Using the measured (0,1,0), (0,2,0), and (0,0,1) energies and $V_0 = 3.7$ cm^{-1}, initial values for ω_2, x_{22}, and ω_3 were determined.

With increasing energy, the next reasonably intense peak occurs at 65.1 cm^{-1}, just under twice the frequency of the short axis bend, and is assigned to (2,0,0), consistent with our earlier assignment.[11] While several levels are expected to occur in this region, *ab initio* calculations for the closely related $S_1 \leftarrow S_0$ absorption predict (2,0,0) to be the most intense,[10] supporting this assignment. ω_1 and x_{11} are uniquely determined from the short axis bend fundamental and overtone frequencies.

The next set of features of reasonable intensity is the pair at 79.2 and 88.1 cm^{-1}. These bands are ~42 cm^{-1} above the (0,2,0)/(0,0,1) Fermi resonance pair, suggesting that they are associated with the stretch overtone and its associated Fermi resonance interaction, which involves the triad (0,4,0), (0,2,1), and (0,0,2). This is confirmed by the dispersed fluorescence spectrum from the (0,0,1) level in S_1, which also shows these two features (see Fig. 2). The ω_2, x_{22}, and ω_3 values determined at the stretch fundamental predict the perturbed levels to occur at 81.2 cm^{-1} and 91.0 cm^{-1} for (0,2,1) and (0,0,2),

respectively, close to where they are observed. The calculations slightly overestimate the energies because they omit the diagonal anharmonic term for the stretch, x_{33}, and the long axis bend – stretch cross anharmonicity, x_{23}. Using the experimental values for the (0,1,0), (0,2,0), (0,0,1), (0,2,1), and (0,0,2) energy levels, the constants ω_2, x_{22}, and ω_3 were refined and values for x_{33} and x_{23} determined, with V_0 remaining fixed at 3.7 cm^{-1}.

At this point in the analysis values have been obtained for eight of the ten constants (ω_1, ω_2, ω_3, x_{11}, x_{22}, x_{33}, x_{23}, and V_0). Values have not been obtained for x_{12} or x_{13}. On this basis we expect that states involving only mode 1 (short axis bend) or involving only modes 2 (long axis bend) and 3 (stretch) and their overtones and combinations can be predicted with reasonable accuracy. Combinations of mode 1 with modes 2 and/or 3 are expected to be less accurately predicted (and overestimated) because of the omission of x_{12} and x_{13}. Thus the levels that we expect to be most accurately predicted are those associated with the next, i.e., second, stretch overtone region and the higher overtones of mode 1.

The second stretch overtone region involves a quartet of anharmonically coupled levels (0,6,0), (0,4,1), (0,2,2), and (0,0,3). The constants predict the two most intense peaks in this region to be at 118.8 cm^{-1} and 129.3 cm^{-1}. Bands are observed at 118.7 cm^{-1} and 128.7 cm^{-1}, close to the predicted values, and are assigned to the perturbed (0,2,2) and (0,0,3) levels, respectively. By fitting to the position of all of the observed transitions involving the stretch/bend Fermi resonance and the bend fundamental, we obtained refined values for ω_2, x_{22}, ω_3, x_{33}, x_{23}, and V_0.

The (3,0,0) and (4,0,0) higher overtone levels of mode 1 are predicted to occur at 94.2 and 121.0 cm^{-1}, respectively. A band is observed at 122.0 cm^{-1} which corresponds closely to the expected band position for (4,0,0). Examination of all predicted levels in the region near 120 cm^{-1} supports the 122.0 cm^{-1} band being associated with (4,0,0), necessitating a small modification to the ω_1 and x_{11} constants. It is not clear that (3,0,0) will be observed, since odd changes in this nontotally symmetric mode are forbidden. However, given that the symmetry forbidden transition to (1,0,0) is observed we consider whether a similar mechanism could impart weak intensity to (3,0,0). The magnitude of the third-order effect associated with the libration mechanism described by Maxton *et al.*[4] can be calculated and is $\sim 10^{-8}$. Clearly, if this mechanism is responsible for providing intensity to the transition to (3,0,0) it will be too weak to be observed. With the improved constants, (3,0,0) is predicted to occur at 94.6 cm^{-1}, while the closest observed bands are at 93.2 and 96.3 cm^{-1}. These are sufficiently far from the predicted value that neither could be assigned to (3,0,0), consistent with the transition being too weak to be observed.

At this point most of the bands observed have been assigned. There are two weak features, at 53.8 cm^{-1} and 74.0 cm^{-1}, occurring at sufficiently low energy and vibrational state density that they should be assignable. We consider the lower band first. Assigning the 53.8 cm^{-1} band turns out to be unexpectedly problematic. It can be assigned to either (1,1,0) or (0,3,0) which, on the basis of the constants determined to this point, are predicted to occur at 55.9 and 52.4 cm^{-1}, respectively. The former is expected to be too high because the cross anharmonicity x_{12} has not been included. To begin we assigned the band to (0,3,0) and adjusted the parameters in a global fit to all of the assigned bands. This led to the quality of the fit deteriorating significantly. The 1.4 cm^{-1} difference between the calculated (0,3,0) band position and the observed band leads to ω_2 and x_{22} being adjusted in the fit and, consequently, ω_3, x_{33}, and x_{23} change as the fit tries to match the observed Fermi resonance band positions at the stretch fundamental and overtones. The substantial reduction in the quality of the fit leads us to conclude that the assignment of the 53.8 cm^{-1} band to (0,3,0) is incorrect. Consequently, it is assigned to (1,1,0). This gives a value for x_{12} and requires no change in the other parameters.

In this context it is interesting to note that Bieske *et al.* observed a weak feature at 49.5 cm^{-1} in the corresponding $S_1 \leftarrow S_0$ REMPI spectrum.[14,21] Believing that this feature may be the absorption analogue of the 53.8 cm^{-1} emission band, to confirm its identity, and hence our corresponding S_0 assignment, we tried to observe this band and measure dispersed fluorescence from it. Unfortunately, we were unable to locate the band using 2D-LIF,[11–13] although we did observe the $\overline{s_0^1}$ absorption transition of the ^{13}C isotopomer 4.0 cm^{-1} to higher energy of the corresponding ^{12}C band. Given that Bieske *et al.* reported the band to have ~5% of the intensity of the stretch feature, our observation of the ^{13}C isotopomer indicates that we had sufficient sensitivity. It appears that the weak feature observed by Bieske *et al*. is an artefact.

Turning now to the 74.0 cm^{-1} band, the only viable assignment using the constants so far determined is (1,0,1), although it is calculated to be some 5 cm^{-1} higher in energy. This level is in Fermi resonance with (1,2,0) and the pair of states must be included in the calculations. The only new parameter necessitated by the inclusion of this pair is x_{13}; the remaining constants can be fixed for the calculation. It emerged that, because of the zero-order position of the (1,2,0) state, the perturbed (1,0,1) level could not go as low as 74.0 cm^{-1}. Consequently, we reversed the ordering of the zero-order (1,2,0) and (1,0,1) levels, which assigned the 74.0 cm^{-1} level as the perturbed (1,2,0) state. The perturbed (1,0,1) level is calculated to be at 66.3 cm^{-1} and consequently it lies beneath the band at 65.1 cm^{-1} associated with the transition terminating in (2,0,0).

2. Spectral assignments based on the spectroscopic constants

At this point 12 of the 16 energy levels extracted from the fit to the spectrum have been assigned. The positions of these 12 energy levels are given in terms of 10 constants: the three harmonic frequencies (ω_1, ω_2, ω_3), the three diagonal anharmonicity constants (x_{11}, x_{22}, x_{33}), the three cross anharmonicity constants (x_{12}, x_{13}, x_{23}), and the cubic anharmonic coupling constant between the stretch and long axis bend (V_0). The constants are summarised in Table II and the calculated and observed band positions are shown in Table I. The constants predict the observed band positions to better than the

TABLE II. Fitted vibrational constants for the S_0 van der Waals vibrational modes of fluorobenzene-argon.

Parameter[a]	Value/cm^{-1}
ω_1	34.7
x_{11}	−1.05
ω_2	23.9
x_{22}	−1.60
ω_3	42.3
x_{33}	−0.48
x_{12}	−2.15
x_{13}	−5.91
x_{23}	−2.59
V_0	3.8

[a]Mode 1 refers to the short axis bend, mode 2 to the long axis bend, and mode 3 to the stretch.

experimental uncertainty of ±0.1 cm^{-1}, with a root-mean-squared deviation of 0.04 cm^{-1}. Where the states are involved in the Fermi resonance, we have listed the calculated linear combination of zero-order states associated with the level. It can be seen that the mixing is extensive and the initial states are spread across the eigenstates. In this situation, assignment to a single zero-order state is somewhat meaningless.

There are four weak bands at 93.2, 96.3, 99.2, and 101.7 cm^{-1} that were extracted from the fit to the $\overline{0^0}$ emission spectrum and have yet to be assigned. These four levels contribute to a weak, broad feature between 92 and 102 cm^{-1} and represent the minimum set of bands required to fit this feature. Given how weak they are and their overlapped nature, one cannot be too trusting of the values extracted. Nevertheless, since the constants allow the positions of various overtones and combinations to be predicted, we have examined possible assignments for these bands. While the density of states increases rapidly, the constants predict the levels to "clump" in certain regions. Four bands, corresponding to the zero-order states (0,3,1), (1,1,1), (2,0,1), and (3,0,0), are predicted to occur between 91 and 95 cm^{-1}, with a gap to another four levels, corresponding to the zero-order states (0,4,1), (2,2,0), (1,2,1), and (2,3,0), between 100 and 104 cm^{-1}. Given the number of states and lack of exact matches to the extracted energies, it is not possible to be definitive in assigning the bands observed. The lack of precise matches suggests that the constants may require further refinement (this is particularly the case where they were based on a single band with low quanta, since the anharmonic corrections depend quadratically on the number of quanta) or may indicate the role of higher order anharmonic coupling coming into play as the state density rises and the separation between states becomes small.

In addition to predicting the band positions, the calculations predict the relative intensities within each Fermi polyad, assuming that only one of the zero order states carries oscillator strength. In the case of the resonances observed, the stretch and its overtones are expected to carry the oscillator strength within each polyad. For the various pairs observed, the observed and calculated intensity ratios are as follows: (0,0,1):(0,2,0) observed 0.63, calculated 0.90; (0,0,2):(0,2,1) observed 2.41, calculated 1.24; (0,0,3):(0,2,2) observed 1.61, calculated 1.11. Qualitatively, the trends calculated match those observed, although there are clear differences at the quantitative level. These differences suggest that the bend states also carry some oscillator strength, leading to enhancement or interference between the two for the various eigenstates. The change in relative intensities seen in emission from $\overline{0^0}$ and $\overline{s^1}$ support this proposition. The transition to the perturbed (0,2,1) level is stronger than the transition to the perturbed (0,0,2) level in emission from $\overline{0^0}$ while the reverse is the case for emission from $\overline{s^1}$. This change would not occur if only the stretch and its overtones carried oscillator strength.

3. Comparison with ab initio calculations

The two most recent *ab initio* studies of S_0 FB-Ar have reported van der Waals vibrational levels up to 75 cm^{-1} (Ref. 8) and 70 cm^{-1} (Ref. 9). While we do not observe all of the levels up to this energy, the constants we have determined allow them to be calculated. The states determined from our spectroscopically derived constants are compared with the *ab initio* determined levels in Table III. Several key observations emerge from this comparison. First, there is generally a good correlation between the *ab initio* calculated energies and those determined from our constants. The key exceptions to this are the high overtones of the long axis bend (although they are not assigned as such by Fajín *et al.*, as discussed below), whose positions determined from the spectroscopic constants are increasingly below the *ab initio* calculated energy. This is to be expected since these levels are not observed and hence the constants are not fitted to them: the quadratic dependence of the changes in energy and coupling constant with vibrational quanta magnify small errors for these high quanta levels. The differences most likely indicate an inadequacy of both the harmonic oscillator-based quantum dependence of the coupling constant and the simple ω_2, x_{22} based approach used to calculate the zero-order energy. Second, small differences in energy in regions where there are several states lead to the ordering of the states being different using our constants compared with the *ab initio* calculations. Third, while the energies generally match well, the assignments of the levels can appear to be quite different at the higher energies. This is largely a consequence of the Fermi resonance. Due to the stretch-bend coupling, the zero-order states (i.e., the combinations and overtones of the simple bend and stretch modes) are substantially mixed and the molecular eigenstates can take on the character of several zero-order states. Differences in assignment largely stem from assigning a level to a different zero-order state within the same Fermi resonance. For example, state number 9 has been assigned by both us and Fajín *et al.*[8] as (1,0,1) while Makarewicz[9] assigns it to the other member of the Fermi resonance pair, (1,2,0). Our assignments are based on the initial zero-order character of the state (based on its position in the coupling matrix) and our calculated linear combination for state number 9 (see Table I) reveals almost equal mixing between (1,0,1) and (1,2,0). Thus either assignment is reasonable but inadequate: assignment to a single zero-order state has little meaning given the significantly mixed character of the states.

All but one assignment (state number 11) is rationalised by recognising the mixed character of the states within a

TABLE III. A comparison between the vibrational levels of S_0 fluorobenzene-argon calculated by *ab initio* methods and those calculated using the spectroscopic constants determined in this work (see Table II). The top group of states are the A′ levels while the bottom group are the A″ levels.

	This work		Fajín *et al.*[d]		Makarewicz[e]	
Level number[a]	Energy/cm^{-1} [b]	Assignment[c]	Energy/cm^{-1}	Assignment	Energy/cm^{-1}	Assignment
0	0	(0, 0, 0)	0	(0, 0, 0)	0	(0, 0, 0)
1	22.3	(0, 1, 0)	22.0	(0, 1, 0)	21.9	(0, 1, 0)
3	37.8	(0, 2, 0)	37.1	(0, 2, 0)	37.6	(0, 2, 0)
4	45.4	(0, 0, 1)	44.4	(0, 0, 1)	45.2	(0, 0, 1)
6	*52.5*	(0, 3, 0)	53.3	(0, 3, 0)	53.9	(0, 3, 0)
7	*66.3*	(0, 1, 1)	62.9	(0, 1, 1)	64.7	(0, 1, 1)
8	65.2	(2, 0, 0)	64.6	(2, 0, 0)	65.4	(2, 0, 0)
10	*63.4*	(0, 4, 0)	68.7	(0, 0, 2)	69.3	(0, 4, 0)
12	*71.1*	(0, 5, 0)	74.4	(0, 1, 2)		
2	33.6	(1, 0, 0)	33.2	(1, 0, 0)	33.4	(1, 0, 0)
5	53.8	(1, 1, 0)	52.7	(1, 1, 0)	53.2	(1, 1, 0)
9	*66.3*	(1, 0, 1)	65.8	(1, 0, 1)	67.0	(1, 2, 0)
11	74.0	(1, 2, 0)	71.8	(1, 1, 1)		

[a]The level numbers are those introduced by Fajín *et al.* (Ref. 8).
[b]Values in italics indicate states that are not observed in the spectrum.
[c]States involved in Fermi resonances are labelled as the zero order state from which the molecular state is derived (see Table I).
[d]CCSD(T) *ab initio* calculations by Fajín *et al.* (Ref. 8).
[e]MP2 *ab initio* calculations by Makarewicz (Ref. 9).

Fermi polyad and realising that any of the states within a polyad may have been used as the assignment for the calculated wavefunction. We have assigned state number 11 to the (1,2,0) level, which is Fermi paired with state number 9, (1,0,1), while Fajín *et al.*[8] have assigned it to (1,1,1) which is Fermi paired with (1,3,0). We suggest that this is a misassignment on their part arising from the difficulty of inferring vibrational quanta from the atomic displacements associated with the calculated vibrational wavefunction. Our constants predict both of the mixed states associated with (1,3,0) and (1,1,1) to be at much higher energies: 79.1 and 92.5 cm^{-1}.

Over the range of vibrational energies studied, the match between the observed and *ab initio* values is sufficiently good that there is no obvious area in which the calculations require improvement, although it is interesting to note that, with the exception of states with high quanta in the long axis bend, the calculations tend to marginally underestimate the observed vibrational energies. It will be interesting to see how the comparisons track when *ab initio* calculations are extended to higher energies.

The *ab initio* calculations have not reported emission intensities, however, $S_1 \leftarrow S_0$ absorption intensities have been reported[10] and these can be used to identify any anomalies. Comparing the intensities qualitatively suggests that the main issue concerns transitions terminating in A″ levels, i.e., those involving odd quanta in mode 1, the short axis bend. Odd quanta changes in this mode are forbidden if the complex is regarded as having C_s point group symmetry. We have noted earlier that the intensity for these transitions involves a different mechanism[4,18] to the case for states involving the long axis bend and stretch, which are both allowed in C_s. There are several bands that we assign as terminating in A″ levels, which requires that they have more intensity than predicted by the calculations for absorption. This is consistent with our earlier observation when comparing the observed and calculated intensities in absorption.[11]

An important issue for comparing *ab initio* calculations with experimental analysis is highlighted by the comparisons and discussion above. When the states are strongly mixed, the extraction of the coefficients for the wavefunction expressed as a linear combination of zero-order states is an important experimental aim. Energies alone provide an incomplete comparison. We suggest that when resonances are present, comparisons between the *ab initio* and experimental results would be enhanced if theoretical methods could be developed that describe the calculated wavefunctions in terms of linear combinations of spectroscopically appropriate zero-order states, since this is the type of information that is extracted from experimental analysis. It would allow a more detailed comparison between the calculations and experimental results, helping to identify areas where calculations could be improved.

B. The FB-Ar$_2$ (1|1) van der Waals vibrations

The discussion above has shown that there is a strong coupling between the stretch and long axis bend overtone in FB-Ar, consistent with the proposal by Bieske *et al.*[14] that such an interaction, caused by a cubic kinetic coupling mechanism, is ubiquitous in aromatic-rare gas complexes. This led us to explore the interaction in the trimer FB-Ar$_2$ (1|1) complex where it should also be manifest.

In our 2D-LIF study of FB-Ar$_2$ (1|1) we reported the observation of a feature at 35.0 cm^{-1} in S_0, which we assigned to the symmetric stretch.[11] We have examined the dispersed fluorescence spectrum afresh at higher resolution, focussing on emission from the $\overline{\overline{0^0}}$ level in the region of the van der Waals modes. The spectrum is shown in Fig. 3. With higher resolution, the single feature reported previously is seen to be composed of two close-lying, overlapped bands. Fitting the

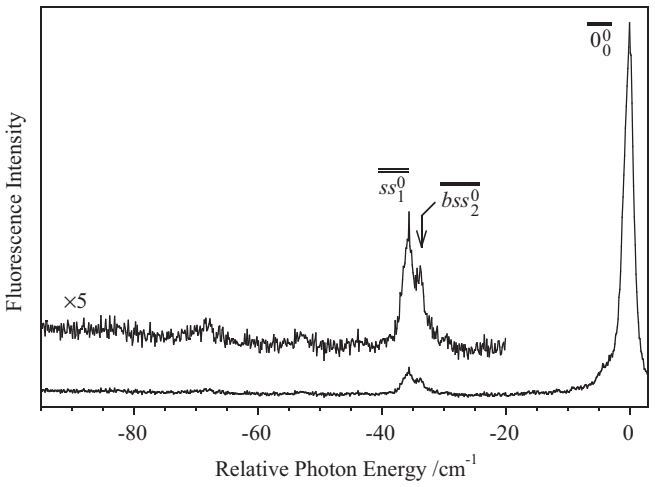

FIG. 3. The dispersed fluorescence spectrum recorded from the $\overline{\overline{0^0}}$ level of FB-Ar_2 (1|1) following excitation of the 0_0^0 transition at 37767.4 cm^{-1}. The spectrum is displayed as displacement from the excitation position to show the vibrational wavenumber associated with the terminating S_0 levels. The assignments represent transitions involving zero-order states (see text for details). The spectrum was measured with a FWHM resolution of 0.6 cm^{-1}.

observed contour reveals the two bands to be at −33.7 and −35.8 cm^{-1}. In addition to this dominant feature, there are a number of weak features evident.

To assign the trimer spectrum, we need to understand how the vibrations and coupling observed for the dimer translate into those of the trimer. There are few reports of the intermolecular vibrations of aromatic-Rg_2 (Rg = rare gas) (1|1) trimers. Bieske, Rainbird, and Knight observed the S_1 van der Waals modes of aniline-Ar_2 (Ref. 15) and, assuming that the second Ar occupies an equivalent position to the first, related the observed trimer frequencies to those of the aniline-Ar dimer. Subsequently, Maxton *et al.* reported intermolecular vibrations for a number of complexes in S_0 using Raman spectroscopy, including benzene-Ar_2 and fluorene-Ar_2 (Ref. 4). Like Bieske *et al.*, they presented a framework for determining intermolecular vibrational frequencies for the trimer, although their considerations were restricted to the Raman active intermolecular bend modes involving libration of the aromatic. Phenol-Ar_2 provides a recent example where the S_1 vibrational structure of an aromatic-Rg_2 trimer has been observed.[22,23]

The formulae provided by Bieske *et al.* allow the six FB-Ar_2 (1|1) intermolecular vibrational frequencies to be calculated from the three FB-Ar intermolecular frequencies and various constants associated with the complex.[15] (The six FB-Ar_2 (1|1) intermolecular modes are the symmetric and asymmetric motions associated with the long axis bend, short axis bend, and the stretch – see Table IV.) The formulae for the trimer (1|1) frequencies in terms of the FB-Ar dimer frequencies are of the general form:

$$\nu_{trimer} = \nu_{dimer}\sqrt{\frac{\mu_{dimer}}{\mu_{trimer}}},$$

where the values for ν_{dimer}, μ_{dimer}, and μ_{trmer} depend on the particular vibration. μ is the effective reduced mass. ν_{dimer} and μ_{dimer} are the same for a particular symmetric/anti-symmetric pair of trimer vibrations. The expressions for μ_{dimer} and μ_{trimer} are shown in Table IV. They depend on parameters that are readily extracted from existing experimental data. I_x and I_y are moments of inertia determined from the FB ground state rotational constants: I_x is determined from A and I_y from B (Ref. 24). The value for the van der Waals bond length, R_0, is that determined from the FB-Ar rotational constants extracted from the microwave spectrum.[25] With these values and the FB and Ar masses, we have determined a set of FB-Ar_2 (1|1) vibrational frequencies based on FB-Ar values of 22.3, 33.7, and 41.8 cm^{-1} for the long axis bend, short axis bend and stretch, respectively. The bend values are those observed, while the stretch value is that obtained by de-perturbing the Fermi resonance. Strictly, the harmonic frequencies should be used for this calculation, however for the purpose of this comparison we have simply used the fundamental frequencies. The calculated set of FB-Ar_2 (1|1) frequencies is shown in Table IV.

TABLE IV. Calculated intermolecular vibrational frequencies of the FB-Ar_2 (1|1) complex based on the FB-Ar van der Waals mode frequencies observed.

	Frequency calculation parameters[a]				
Vibrational mode	ν_{dimer}	μ_{dimer}[c]	μ_{trimer}[c]	Calculated frequency/cm^{-1}	Symmetry[b]
Symmetric stretch ν_{ss}	ν_s	$\left(\frac{1}{m_{Ar}}+\frac{1}{m_{FB}}\right)^{-1}$	m_{Ar}	35.1	a_1
Asymmetric stretch ν_{sa}	ν_s	$\left(\frac{1}{m_{Ar}}+\frac{1}{m_{FB}}\right)^{-1}$	$\left(\frac{1}{m_{Ar}}+\frac{2}{m_{FB}}\right)^{-1}$	47.6	b_1
Symmetric short axis bend ν_{bss}	ν_{bs}	$\left(\frac{1}{m_{Ar}R_0^2}+\frac{1}{m_{FB}R_0^2}+\frac{1}{I_x}\right)^{-1}$	$\left(\frac{1}{m_{Ar}R_0^2}+\frac{2}{m_{FB}R_0^2}\right)^{-1}$	17.1	b_2
Asymmetric short axis bend ν_{bsa}	ν_{bs}	$\left(\frac{1}{m_{Ar}R_0^2}+\frac{1}{m_{FB}R_0^2}+\frac{1}{I_x}\right)^{-1}$	$\left(\frac{1}{m_{Ar}R_0^2}+\frac{2}{I_x}\right)^{-1}$	44.5	a_2
Symmetric long axis bend ν_{bls}	ν_{bl}	$\left(\frac{1}{m_{Ar}R_0^2}+\frac{1}{m_{FB}R_0^2}+\frac{1}{I_y}\right)^{-1}$	$\left(\frac{1}{m_{Ar}R_0^2}+\frac{2}{m_{FB}R_0^2}\right)^{-1}$	15.1	a_1
Asymmetric long axis bend ν_{bla}	ν_{bl}	$\left(\frac{1}{m_{Ar}R_0^2}+\frac{1}{m_{FB}R_0^2}+\frac{1}{I_y}\right)^{-1}$	$\left(\frac{1}{m_{Ar}R_0^2}+\frac{2}{I_y}\right)^{-1}$	27.7	b_1

[a] $\nu_{trimer} = \nu_{dimer}\sqrt{\mu_{dimer}/\mu_{trimer}}$.

[b] Based on the complex being assigned to the C_{2v} point group.

[c] m_{Ar} denotes the mass of Ar; m_{FB} denotes the mass of FB; R_0 is the distance from the FB plane to the Ar atom; I_y is the moment of inertia for rotation of FB about the in-plane axis that lies perpendicular to the direction of the long axis vibration (We have labelled this short axis vibration direction the *y*-axis; the long axis direction is labelled *x*.); I_x is the moment of inertia for rotation of FB about the in-plane axis that lies parallel to the direction of the long axis vibration.

Bieske *et al.* also provided expressions relating the cubic anharmonic coupling terms in the dimer and trimer species.[15] The formulae are of the general form:

$$V_{trimer} = \frac{1}{\sqrt{2}} \left(\frac{\mu_s^{dimer}}{\mu_s^{trimer}}\right)^{1/4} \left(\frac{\mu_b^{dimer}}{\mu_b^{trimer}}\right)^{1/2} V_{dimer},$$

where V represents the cubic coupling constant in the dimer or trimer, μ_s^{dimer} refers to μ_{dimer} for the stretch, μ_b^{dimer} refers to μ_{dimer} for the appropriate bend direction, and similarly for the trimer values. The μ values are tabulated for each of the vibrations in Table IV. These formulae allow the interactions between the various stretch and bend levels in the trimer to be deduced from those in the dimer and *vice versa*.

Based on these calculated frequencies and assigning the complex to the C_{2v} symmetry point group, there are four bands with the correct symmetry to be seen below 40 cm^{-1}. These are $\overline{\overline{bls}}_1^0$ at −15.1 cm^{-1}, $\overline{\overline{bls}}_2^0$ at −30.2 cm^{-1}, $\overline{\overline{bss}}_2^0$ at −34.2 cm^{-1}, and $\overline{\overline{ss}}_1^0$ at −35.1 cm^{-1}, where the values quoted are shifts from the $\overline{\overline{0}}_0^0$ band and we have not made any allowance for anharmonicity in calculating the positions of the bend overtones. Both of the bend overtones are expected to be weak due to unfavourable Franck-Condon factors. Based on the calculated frequencies, the features observed in the spectrum at −33.7 and −35.8 cm^{-1} can be securely assigned to $\overline{\overline{bss}}_2^0$ and $\overline{\overline{ss}}_1^0$, respectively. Since $\overline{\overline{bss}}_2^0$ is not expected to be a strong feature, the observation that it is approximately half as intense as $\overline{\overline{ss}}_1^0$ suggests that the two terminating states are in Fermi resonance. Interestingly, this resonance involves the stretch and short axis bending direction: coupling involving these motions was not observed in the dimer due to the high frequency of the bend, which made the energy separation between the stretch and short axis bend overtone very large (>20 cm^{-1}). Analysis of the interaction in the trimer provides a means to predict the value for the dimer.

Before considering this, however, we examine the situation for the resonance that was observed for the dimer, involving the stretch and long axis bend motion. Given the observation of $\overline{\overline{ss}}_1^0$ at −35.8 cm^{-1}, the nearest level involving long axis bending that can couple to ν_{ss} is $2\nu_{bls}$, which is predicted to occur at −30.2 cm^{-1}. Using the V_0 value of 3.8 cm^{-1} determined for the $\nu_s - 2\nu_{bl}$ coupling in the dimer, Bieske, Rainbird, and Knight's formula (see above) predicts a coupling matrix element of 1.7 cm^{-1} for the $\nu_{ss} - 2\nu_{bls}$ interaction. With this predicted coupling matrix element and energy separation, the $\overline{\overline{bls}}_2^0$ band is calculated to have ∼10% of the $\overline{\overline{ss}}_1^0$ intensity. Careful examination of Fig. 3 indicates a weak feature at −29.5 cm^{-1}. A fit to the $\overline{\overline{ss}}_1^0 - \overline{\overline{bss}}_2^0$ pair including this feature gives it an intensity of 10% of the $\overline{\overline{ss}}_1^0$ band, consistent with expectations. On this basis we assign it to the $\overline{\overline{bls}}_2^0$ band.

Returning to the $\nu_{ss} - 2\nu_{bss}$ interaction, a complete analysis of the resonance should include the three levels ν_{ss}, $2\nu_{bss}$, and $2\nu_{bls}$ since, while the $\nu_{ss} - 2\nu_{bls}$ interaction does not lead to significant intensity changes, the energy shifts involved could potentially influence the near-resonant $\nu_{ss} - 2\nu_{bss}$ interaction. To assess the effect, we have analysed it as both a two and three level system. Using the relative intensities and energy separations extracted from the fit to the spectrum, deconvoluting the interaction involving $\nu_{ss} - 2\nu_{bss}$ as a simple two level system gives unperturbed energies of $2\nu_{bss}$ = 34.5 cm^{-1} and ν_{ss} = 35.0 cm^{-1} with a $\nu_{ss} - 2\nu_{bss}$ coupling matrix element of 1.0 cm^{-1}. Adding the $\nu_{ss} - 2\nu_{bls}$ interaction and deconvoluting it as a three level system (again, based on the band positions and relative intensities extracted from the fit) using the Green's function deconvolution procedure of Lawrance and Knight[26] yields zero-order energies for $2\nu_{bls}$, $2\nu_{bss}$, and ν_{ss} of 29.8, 34.5, and 34.7 cm^{-1}, respectively, and coupling matrix elements of 1.2 and 1.1 cm^{-1} for $\nu_{ss} - 2\nu_{bls}$ and $\nu_{ss} - 2\nu_{bss}$, respectively. The inclusion of the second interaction has only had a minor influence on the $\nu_{ss} - 2\nu_{bls}$ coupling matrix element extracted (it increases by 4%) while the separation between the corresponding zero-order states decreases from 0.5 cm^{-1} to 0.2 cm^{-1}. The $\nu_{ss} - 2\nu_{bls}$ coupling value of 1.2 cm^{-1} extracted from the deconvolution is somewhat lower than the 1.7 cm^{-1} that the Bieske, Rainbird and Knight[15] formula predicts but, in view of how weak the $\overline{\overline{bls}}_2^0$ band is and the poor signal to noise ratio, the match is satisfactory.

Using the formula of Bieske *et al.*,[15] the coupling matrix element for the $\nu_s - 2\nu_{bs}$ interaction in the dimer is calculated from the $\nu_{ss} - 2\nu_{bss}$ trimer interaction to be 3.2 cm^{-1}. This is quite close to the value of 3.8 cm^{-1} determined for the $\nu_s - 2\nu_{bl}$ interaction. The similarity in these values may be an indication of the kinetic coupling mechanism[27] as suggested by Bieske *et al.*[14]

As noted above, there are several weak features that are just discernable in the spectrum. Given the observed dimer bands and predicted trimer frequencies, it is interesting to see whether there are tentative assignments for them. The normally symmetry forbidden A″ short axis bend fundamental was prominent in the dimer and its intensity was a close match to that expected based on the libration mechanism proposed by Maxton *et al.* This mechanism predicts that the asymmetric short axis bend fundamental will be seen in the trimer and there is evidence for a very weak feature at −43.8 cm^{-1}, which compares well with the predicted frequency of ν_{bsa} of 44.5 cm^{-1}. The more clearly observed feature at −53.0 cm^{-1} matches the position where the asymmetric long axis bend overtone is expected (−55.4 cm^{-1}). There is also evidence for a sequence of close-lying bands in the region around 68 cm^{-1}. These correspond to where one expects to see the symmetric stretch overtone and its associated Fermi interactions.

While the comparison with observed bands is limited, the formulae of Bieske *et al.*[15] appears to provide satisfactory estimates of the intermolecular vibrational frequencies in the (1|1) complex.

V. CONCLUSIONS

We have measured dispersed fluorescence spectra from the $\overline{0^0}$ and $\overline{s^1}$ levels of fluorobenzene-Ar. The $\overline{0^0}$ spectrum reveals S_0 van der Waals mode vibrational structure up to ∼130 cm^{-1}, encompassing some three orders of magnitude in intensity range. The spectrum was fitted to identify the

spectral bands while accounting for grating ghosts, with sixteen bands extracted. Twelve of these were assigned based on a set of 10 constants that included the harmonic frequencies and anharmonic constants, and a strong Fermi resonance between the stretch and long axis bend overtone that becomes quite ubiquitous at high energies. The Fermi resonance leads to strong mixing among the zero-order states and this makes assignment in terms of the simple bend and stretch motions largely meaningless for these states. The constants provide an excellent match with the experimental energies but, while the calculated relative intensities within a Fermi polyad determined by assuming the stretch carries all of the oscillator strength qualitatively match those observed, there is not a quantitative match. This, along with differences between the relative intensities seen in emission from $\overline{0^0}$ and $\overline{s^1}$, suggests that the bend overtone and stretch/bend overtone combination levels also carry oscillator strength. Comparison between the energy levels we calculate from the spectroscopic constants and those calculated by *ab initio* methods generally reveals a good match. There is a trend for the spectroscopic constants to underestimate the energies of high overtones of the long axis bend. The assignments reported for these states differ amongst various authors but this is simply a consequence of different members of a Fermi polyad being identified. This illustrates that any attempt to label the states in terms of simple stretch/bend motions and their combinations and overtones is fraught. Nevertheless, this does highlight an issue for comparing *ab initio* calculations with experimental results in such circumstances. We ponder whether theoretical methods could be developed to better describe the calculated wavefunctions as linear combinations of simple bend and stretch overtones and combinations, which is the type of information that is extracted from experimental analysis.

The availability of these experimental data presents an opportunity to extend *ab initio* calculations to higher vibrational energies to provide an assessment of the accuracy of the calculated potential surface away from the minimum. Because of the difficulties in assigning spectral features to particular vibrational states due to both the increasing state density and the mixed character of states involved in the Fermi resonance, it would be useful for intensities to be included in such calculations.

The dispersed fluorescence spectrum from the $\overline{\overline{0^0}}$ level of FB-Ar_2 (1|1) was also measured. The spectrum is dominated by two overlapped features, which we have assigned as a Fermi resonance-mixed pair involving the symmetric short axis bend overtone and the symmetric stretch. The observation of this interaction allowed us to extract a value for the stretch-short axis bend overtone interaction in the dimer. Interestingly, the cubic coupling matrix elements are quite similar for the interactions between the stretch and long and short axis bend overtones. This is consistent with the proposal by Bieske *et al.*[14] that such an interaction is caused by a cubic kinetic coupling mechanism and is ubiquitous in aromatic-rare gas complexes. The vibrational frequencies predicted by the formula of Bieske *et al.*[15] enable a number of the weak features in the spectrum to be identified.

ACKNOWLEDGMENTS

We thank the School's Electronic and Mechanical workshop staff for their support in constructing and maintaining the apparatus. This research was supported by the Australian Research Council and Flinders University.

[1] K. S. Kim, P. Tarakeshwar, and J. Y. Lee, Chem. Rev. **100**, 4145 (2000).
[2] P. Hobza and K. Müller-Dethlefs, *Non-Covalent Interactions* (Royal Society of Chemistry, Cambridge, 2010).
[3] R. Sussmann and H. J. Neusser, J. Chem. Phys. **102**, 3055 (1995).
[4] P. M. Maxton, M. W. Schaeffer, S. M. Ohline, W. Kim, V. A. Venturo, and P. M. Felker, J. Chem. Phys. **101**, 8391 (1994).
[5] R. Sussmann, R. Neuhauser, and H. J. Neusser, J. Chem. Phys. **103**, 3315 (1995).
[6] R. Neuhauser, J. Braun, H. J. Neusser, and A. Van Der Avoird, J. Chem. Phys. **108**, 8408 (1998).
[7] W. Kim and P. M. Felker, J. Chem. Phys. **107**, 2193 (1997).
[8] J. L. C. Fajín, J. L. Cacheiro, B. Fernandez, and J. Makarewicz, J. Chem. Phys. **120**, 8582 (2004).
[9] J. Makarewicz, J. Chem. Phys. **121**, 8755 (2004).
[10] J. L. C. Fajín, S. B. Capelo, B. Fernandez, and P. M. Felker, J. Phys. Chem. A **111**, 7876 (2007).
[11] J. R. Gascooke, U. N. Alexander, and W. D. Lawrance, J. Chem. Phys. **136**, 134309 (2012).
[12] N. J. Reilly, T. W. Schmidt, and S. H. Kable, J. Phys. Chem. A **110**, 12355 (2006).
[13] J. R. Gascooke, U. N. Alexander, and W. D. Lawrance, J. Chem. Phys. **134**, 184301 (2011).
[14] E. J. Bieske, M. W. Rainbird, I. M. Atkinson, and A. E. W. Knight, J. Chem. Phys. **91**, 752 (1989).
[15] E. J. Bieske, M. W. Rainbird, and A. E. W. Knight, J. Chem. Phys. **94**, 7019 (1991).
[16] K. Rademann, B. Brutschy, and H. Baumgärtel, Chem. Phys. **80**, 129 (1983).
[17] P. Butler, D. B. Moss, H. Yin, T. W. Schmidt, and S. H. Kable, J. Chem. Phys. **127**, 094303 (2007).
[18] R. Sussmann, R. Neuhauser, and H. J. Neusser, Chem. Phys. Lett. **229**, 13 (1994).
[19] G. Herzberg, *Molecular Spectra and Molecular Structure II: Infrared and Raman Spectra of Polyatomic Molecules* (Van Nostrand Reinhold, New York, 1945).
[20] E. B. Wilson, J. C. Decius, and P. C. Cross, *Molecular Vibrations: The Theory of Infrared and Raman Vibrational Spectra* (Dover, New York, 1955).
[21] It is clear by examining other reports (see Table VII in Ref. 11) that the van der Waals vibrational frequencies determined by Bieske *et al.* (Ref. 14) are too high. Bieske *et al.* report a feature at 54 cm^{-1}. We have recalibrated their spectrum and the value of 49.5 cm^{-1} is our recalibrated value for the band position.
[22] I. Kalkman, C. Brand, T. B. C. Vu, W. L. Meerts, Y. N. Svartsov, O. Dopfer, X. Tong, K. Muller-Dethlefs, S. Grimme, and M. Schmitt, J. Chem. Phys. **130**, 224303 (2009).
[23] A. Armentano, X. Tong, M. Riese, S. M. Pimblott, K. Muller-Dethlefs, M. Fujii, and O. Dopfer, Phys. Chem. Chem. Phys. **13**, 6071 (2011).
[24] Z. Kisiel, E. Bialkowska-Jaworska, and L. Pszczolkowski, J. Mol. Spectrosc. **232**, 47 (2005).
[25] W. Stahl and J. U. Grabow, Z. Naturforsch. A **47**, 681 (1992).
[26] W. D. Lawrance and A. E. W. Knight, J. Phys. Chem. **89**, 917 (1985).
[27] E. L. Sibert, J. T. Hynes, and W. P. Reinhardt, J. Phys. Chem. **87**, 2032 (1983).